Chiral/ring closed vs. Achiral/open chain triazine-based organogelators: induction and amplification of supramolecular chirality in organic gels

Luisa Lascialfari, Debora Berti, Alberto Brandi, Stefano Cicchi,* Matteo Mannini, Gennaro Pescitelli,* Piero Procacci.

Electronic Supplementary Information

Experimental section

Technical remarks.

The R_f values refer to aluminum sheets of silica gel 200 μm thick with a granulometry of 10-12 μm and with a fluorescent label. For *flash column chromatography* separation silica gel 60 with a 40-63 μm granulometry was used. Both are provided by Merck.

Melting points were obtained with an apparatus by Electrothermal.

NMR spectra were acquired with Varian Gemini apparatus with a resonating frequency respect to the ^{1}H nucleus of 200MHz, 300MHz or 400MHz. Chemical shift values are expressed in δ(ppm) respect to the tetramethylsilane (TMS) resonating frequency. Notation s, d, t, m, bs are referred to the signal multiplicity, and mean respectively: singlet, doublet, triplet, multiplet, broad signal. The letter *p* before these notations means "pseudo".

IR spectra were recorded with a Perkin-Elmer FT-IR881 spectrophotometer. The frequencies are expressed in wavenumbers ν in cm^{-1}. Notations w, m and s, referred to the signal intensity, mean respectively weak, medium and strong.

For *mass spectrometry* measurements a Shimadzu GCMS-QP5050A Gas Chromatograph Mass Spectrometer with a 70eV Electronic Ionization (EI), or a LCQ-Fleet Thermo Scientific Electron Spry Ionization (ESI) apparatus were used. Intensities are reported in m/z and expressed as percentage respect to the most intense peak.

Elemental analysis were realized with a Perkin-Elmer 240 analyzer.

UV-vis spectra were recorded with a Varian Cary 4000 with sample holders 1mm thick.

Specific rotation for chiral compounds were carried out with a Jasco-DIP370 Polarimeter and were referred to the sodium D line (589 nm). The reported values are the average of 30 measurements.

Circular Dichroism (CD) measurements were performed with a Jasco J-715 spectropolarimeter equipped with a Jasco spectropolarimeter power supply PS-150J and a thermostatic bath Lauda Ecoline RE204. Sample holder consists in a thermostatable quartz cell with a path length of 0.01 cm. All CD spectra resulted from an average of 15 scans and were repeated after rotation of the cell in order to minimize the eventual contribution of LD (Linear Dichroism). All gel samples were prepared with the same procedure, i.e. introducing the boiling solution in the quartz cell and allowing it to cool to r.t. and gelate, since the measure can be affected by differences in the dynamic of gel formation.[1]

Small Angle and Wide Angle X-Ray Scattering (SAXS/WAXS) experiments employed a Hecus X-ray System GMBH Graz S3micro equipped with an ultra brilliant point microfocus source Gemix-Fox 3D (Xenoxs, Grenoble). The scattered X-rays were detected by a two-dimensional position sensitive detector with a sample-to-detector distance of 269 mm. This configuration allow values of the scattering vector q [$Å^{-1}$] in the range $0.0008<q<2.43$. Here q is defined as $q=(4\pi/\lambda)\sin(\Theta/2)$. Samples were prepared in glass capillaries of 2 mm diameter. Hot sample solutions were introduced in the capillary, which was immediately sealed with dual glue, and then allowed to cool and gel. All measurements were collected at room temperature and employing a X-Ray source power of 50W (50 kV, 1mA).

$T_{gel\text{-}sol}$ *and* $T_{sol\text{-}gel}$ measurements were performed with a TA Instrument DSC Q2000 apparatus. Steel sealed pan were used. All results refer to scans with a heating/cooling gradient of 1 °C/min.

For *Atomic Force Microscopy* (AFM) measurements the samples were prepared by dropping 50 μL of gel on a freshly cleaved mica slide (Dumico, Rotterdam, The Netherlands) and directly mounted in the spin-coater (KW 4A Chemat Technology). Spinning has been carried out at 3000 rpm for 60 s. The obtained samples

[1] K. Murata, M. Aoki, T. Suzuki, T. Harada, H. Kawataba, T. Komori, F.Ohseto, K. Ueda, S. Shinkai, *J. Am. Chem. Soc.* **1994**, 116, 6664-6676.

were dried under a dry nitrogen flux and then mounted in the sample holder of the microscope. AFM analysis was performed with a P47-PRO instrument (NT-MDT co. Zelenograd, Moscow, Russia) using a NSC36 silicon tip (MikroMasch, Tallinn, Estonia) having a resonating frequency of 155 kHz and a spring constant of 1,75 N/m. Semicontact mode (tapping mode) was used in order to avoid deformation or damage of the examined soft samples. All the images were processed using the WSXM 4.0 Nanotec software.[2]

Synthesis. Compounds **1a**,[3] **1b**,[3] (S)-**3**[4] **6**,[5] and **8**,[4] were synthesized following the corresponding literature reference.

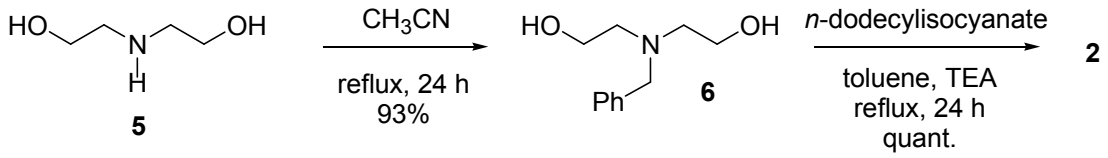

Scheme 1s. Synthesis of compound **2**

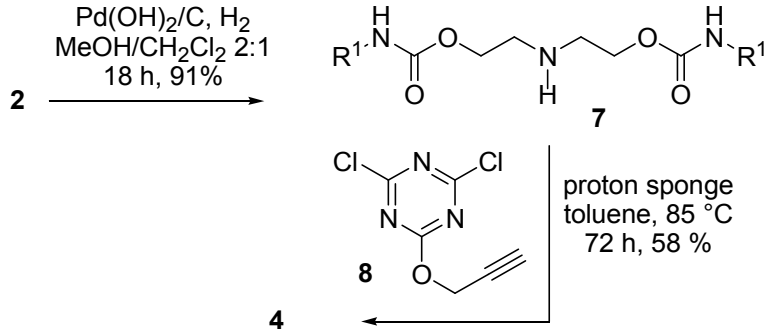

Scheme 2s. Synthesis of compound **4**

Dodecyl-carbamic acid 2-[benzyl-(2-dodecylcarbamoyloxy-ethyl)-amino]-ethyl ester (**2**)

A dry toluene solution (15 mL) of **6** (512 mg, 2.61 mmol, 1 eq), kept under nitrogen atmosphere, was added with *n*-dodecylisocyanate (1.566 g, 7.41 mmol, 1.4 eq, d = 0.877 g/mL) and dry TEA (triethylamine) (52.7 mg, 0.522 mmol, 0.1 eq, 73 µL, d=0.72 g/mL) and refluxed for 24 hours. The solution was then evaporated to dryness and the resulting crude mixture was dissolved in CH_2Cl_2 (100 mL) and washed with brine. The organic layer was dried over sodium sulfate and concentrated. The solid was then purified via flash column chromatography, eluting with polarity gradient starting with CH_2Cl_2 and adding Ethyl Acetate (EtOAc) to give 1.61 g of a white solid. Yield quantitative.

R_f =0.69 (CH_2Cl_2/AcOEt 4:1); Mp = 54-56 °C; ^{1}H NMR (200 MHz, $CDCl_3$): δ = 7.31-7.24 (m, 5H, Ph), 4.95 (bs, 2H, N*H*), 4.11 (t, 4H, ^3J = 5.5 Hz, CH_2O), 3.70 (s, 2H, CH_2Ph), 3.13 (pq, 4H, ^3J = 6.6 Hz, NHCH_2), 2.77 (t, 4H, ^3J = 5.5 Hz, NCH_2), 1.44 (m, 4H, NHCH$_2$CH_2), 1.25 (m, 36H, CH_2 chains), 0.87 (t, ^3J = 6.4 Hz, 6H, CH_3) ppm; ^{13}C NMR (50 MHz, $CDCl_3$): δ = 156.8 (s, 2C, C=O), 139.5 (s, 1C, *C*Ph), 129.0 (d, 2C, *C*H-

[2] a) I. Horcas, R. Fernandez,J.M. Gomez-Rodriguez, J. Colchero, J. Gomez-Herrero, A. M. Baro, *Rev. Sci. Instrum*. **2007**, 78, 013705; b) free download from http://www.nanotec.es/

[3] Cicchi, S.; Ghini, G.; Lascialfari, L.; Brandi, A.; Betti, F.; Berti, D.; Ferrati, S.; Baglioni, P. *Chem. Commun.* **2007**, 1424-1426.

[4] Ghini, G.; Lascialfari, L.; Vinattieri, C.; Cicchi, S.; Brandi, B.; Berti, B.; Betti, FR.; Baglioni, P.; Mannini, M. *Soft Matter* **2009**, *5*, 1863-1869

[5] Saalfrank, R. W.; Deutscher, C.; Sperner, S.; Nakajima, T.; Ako, A.M.; Uller, E.; Hampel, F.; Heinemann, F. W. *Inorg. Chem.*, **2004**, *43*, 4372-4382.

o), 128.4 (d, 2C, *C*H-m), 127.2 (d, 1C, *C*H-p), 63.4 (t, 2C, *C*H_2-O), 60.1 (t, 1C, *C*H_2-Bn), 53.5 (t, 2C, N*C*H_2), 41.5 (t, 2C, NH*C*H_2), 32.4 (t, 2C, NHCH_2*C*H_2), 30.7 (t), 30.4 (t), 30.1 (t), 29.8 (t), 27.2 (t, 16C, CH_2 aliphatic chains), 23.1 (t, 2C, CH_2CH_3), 14.6 (q, 2C) ppm; IR (KBr): ν = 3377, 3314 (s, N-H), 3066, 3028 (w, sp^2 C-H stretching), 2919, 2849 (s, sp^3 C-H stretching), 1688 (s, C=O), 1614 (m, C=C), 1548 (s), 1467 (m), 1498 (m), 1271 (s) cm^{-1}; MS (EI, 70eV): m/z (%)= 619 (0.1) $[M+1]^+$, 618 (0.1) $[M]^+$, 375 (15), 256 (16) $[M\text{-}Bn]^+$, 159 (49), 99 (40), 91 (100) [tropylium cation]; Elemental Analysis Calculated for $C_{37}H_{67}N_3O_4$ (617.95) : C 71.92, H 10.93, N 6.80; Found: C 72.07, H 11.20, N 7.00.

Dodecyl-carbamic acid 2-(2-dodecylcarbamoyloxy-ethylamino)-ethyl ester (**7**)

Compound **2** (584 mg, 0.94 mmol) was dissolved in 15 mL of a 1:2 mixture CH_2Cl_2/MeOH. Then 10 % $Pd(OH)_2$/C (290 mg) was added. The reaction flask was purged with nitrogen and then with hydrogen. The reaction mixture was stirred for 18 hours under a hydrogen atmosphere. Mixture was filtered on celite in order to remove the Pd catalyst. To have a good recovery of the product the celite was washed several times with $CHCl_3$. The collected filtrate was evaporated to dryness. The crude was analyzed via NMR to detect the disappearance of the signal of the benzyl group. After that the crude was dissolved in $CHCl_3$ and washed 3 times with a saturated solution of Na_2CO_3. The organic layer was dried over Na_2SO_4 and concentrated, giving 451 mg of a gummy solid (yield 91%) which was used without further purification.

^{1}H NMR (200 MHz, $CDCl_3$): δ = 4.84 (bs, 2H, NC*H*$_2$), 4.14 (t, 4H, ^3J = 5.1 Hz, OC*H*$_2$), 3.13 (pq, 4H, ^3J = 6.5 Hz CONHC*H*$_2$), 2.85 (pt, ^3J = 4.5 Hz, 4H, NHC*H*$_2$), 1.46 (m, 4H, CONHCH$_2$C*H*$_2$), 1.23 (bm, 36H, CH_2), 0.86 (t, ^3J = 6.4 Hz, 6H, C*H*$_3$) ppm.

Dodecyl-carbamic acid 2-[{4-[bis-(2-dodecylcarbamoyloxy-ethyl)-amino]-6-prop-2-ynyloxy-[1,3,5]triazin-2-yl}-(2-dodecylcarbamoyloxy-ethyl)-amino]-ethyl ester (**4**)

Compound **7** (344 mg, 0.65 mmol, 1.75 eq), compound **8** (39 mg, 0.19 mmol, 1 eq) and proton sponge (1,8-bis(dimethylamino) naphthalene) (139 mg, 0.65 mmol, 1.75 eq) were dissolved in dry toluene (1.3 mL) to realize a 0.5 M concentration of **7**. The mixture was kept at 85 °C under nitrogen atmosphere for 72 hours. The solution was concentrated under vacuum and purified via flash column chromatography to give 131 mg of product as a white solid (yield 58%).

R_f = 0.3 ($CHCl_3$/AcOEt 6:1); Mp = 125-128 °C. ^{1}H NMR (200 MHz, $CDCl_3$): δ = 5.48 (bs, 2H, N*H*), 5.17 (bs, 2H, N*H*),4.86 (d, ^4J = 2.2 Hz, 2H, OC*H*$_2$C≡CH), 4.29 (bs, 8H, OC*H*$_2$), 3.78 (bs, 8H,NC*H*$_2$), 3.11 (bs, 8H, NHC*H*$_2$), 2.44 (t, ^4J = 2.2 Hz, 1H, C≡C*H*), 1.47 (m, 8H, CONHCH$_2$C*H*$_2$), 1.24 (bm, 72H, C*H*$_2$), 0.86 (t, ^3J = 6.3 Hz, 12H, C*H*$_3$) ppm; ^{13}C NMR (50 MHz, $CDCl_3$): δ = 169.4 (s, 1C, *C*-O), 166.0 (s, 2C, *C*-N), 156.7 (s, *C*=O), 156.5 (s, *C*O), 78.9 (s, 1C, *C*≡CH), 74.6 (d, 1C, C≡*C*H), 62.8 (t, 2C, O*C*H$_2$), 62.7 (t, 2C, O*C*H$_2$), 54.1 (t, 1C, O*C*H$_2$), 48.7 (t, 2C, NC*H*$_2$), 48.4 (t, 2C, N*C*H$_2$), 41.4 (t, NH*C*H$_2$), 40.9 (t, NH*C*H$_2$), 32.2, 30.5, 30.2, 29.9, 29.6, 27.1, 23.0, 40C, *C*H$_2$ aliphatic chains, 14.4 (q, 4C, *C*H$_3$) ppm; IR (KBr): ν = 3356 (s, N-H stretching), 3327 (s, N-H stretching), 3066-3028 (m, sp^2 C-H stretching), 2919-2852 (s, sp^3 C-H stretching), 1698 (s, C=O stretching), 1548 (s); MS (ESI): m/z (%)= 1188 (16) $[M+H]^+$, 1210 (100) $[M+Na]^+$, 1226 (14) $[M+K]^+$; Elemental analysis calculated for $C_{66}H_{123}N_9O_9$ (1186.74): C 66.80, H 10.45, N 10.62. Found C 66.95, H 10.33, N 10.73.

Solvent	range of concentration, mg/mL	
	Compound (S)-**3**	Compound **4**
n-hexane	G (10.0)	G (10.0-2.5)
n-hexane/EtOH	G (10.0-2.5)	P
cyclohexane	G (10.0-5.0)	G (10.0-2.5)
cyclohexane/EtOH	G (10.0-2.0)	S
toluene	G (10.0-5.0)	S
xylenes	G (5.0)	S
$(i\text{-Pr})_2O$	G (10.0-2.5)	G (10.0-7.5)
	Mixtures	
	(S)-**3** : **4** (10 : 90)	(S)-**3** : **4** (5:95)
Cyclohexane	G (10.0-2.0)	G (10.0-2.0)

Table 1s. Gelling abilities of compound (S)-**3** and **4** and their mixtures. G= Gel, S= Solution, P=Precipitation

Dynamic Light Scattering

DLS experiments were carried out on a Brookhaven Instrument apparatus equipped with a BI900AT correlator card and BI200 SM goniometer (New York, USA). The light source was the doubled frequency of a Coherent Innova diode pumped Nd-YAG laser, (λ=532nm, 20mW). Measurements were performed at 25 °C on 0.5 ml samples previously transferred into cylindrical Hellma scattering cells. For each sample, the measurement was performed at the scattering angle θ=90 corresponding to the scattering vector

$$|q| = \frac{4\pi n}{\lambda}\sin\left(\frac{\theta}{2}\right)$$

where n is the refractive index of cyclohexane (1.42647).
DLS experiments measure the normalized time autocorrelation function of the intensity of the scattered light, which can be expressed as:

$$g_2(q,t) = A\left[1+\beta^2 g_1\left(q,t\right)^2\right]$$

where A is the measured baseline, β the spatial coherence factor, and $g_1(q,t)$ the normalized electric field correlation function.
For a dilute suspension of monodisperse particles, $g_1(q,t)$ decays exponentially with a decay rate $\Gamma = Dq^2$, where q is the magnitude of the scattering vector, and D is the translational diffusion coefficient, which is related to the hydrodynamic diameter d_h through the Debye-Stokes Einstein relationship:

$$D = \frac{K_B T}{3\pi\eta d_h}$$

where T is the temperature in K, K_B the Boltzmann constant and η is the medium viscosity.
The analysis of the distribution of decay times was performed according to standard procedures, and interpreted through a cumulative expansion of the field autocorrelation function, arrested at the second order.[6]

[6] D. E. Koppel, *J. Chem. Phys.* **1972**, *57*, 4814.

Alternatively the size distribution has been obtained through Laplace inversion of the experimental data, using a constrained regularization method, CONTIN.[7]

[7] S. W. Provencher, *Comput. Phys. Commun*., **1982**, *27*, 229.

Computational section

Molecular dynamics calculations

The force field used in the Molecular Dynamics simulations is based on the AMBER/GAFF parametrization.[8] Atomic charges of compound (S)-**3** and **4** were computed *ab initio* by optimizing the structures at the HF/STO-3G level of theory and then by evaluating the charges at the B3LYP/6-31G(d) level on the optimized structures using the Electrostatic Potential Fit (ESP) scheme by Merz-Singh-Kollman.[9] In building up the model structures of the (S)-**3** and of the mixture (S)-**3** +**4** aggregates, we removed the aliphatic chains at the amide moieties substituting them with a simple methyl group. As supporting material we provide, the HF/STO-3G optimized structured of (S)-**3** and **4** model compounds, along with the force field parameters in text format. The simulation were performed *in vacuo*. The constant temperature of 300 K was enforced using a Nose's thermostat. This simulation protocol should mimic the standard conditions of purely apolar aliphatic solvents such as, e.g. cyclohexane, that are able to solvate the alkyl chains of (S)-**3** and **4** while exhibiting no competing interactions with the solute regarding intermolecular stacking and intermolecular H-bonding. The Nose-Hoover equations of motion for the thermostated systems were integrated using a multiple time step scheme with an external time step of 3 fs and an internal time step of 0.5 fs. All calculations were performed using the program ORAC.[10]

Simulation of 16 units of compound (S)-**3.** The system was prepared by piling up sixteen molecules of compound (S)-**3** with the triazine planes parallelly stacked. The extension of the starting configuration along the axis perpendicular to the triazine planes was of about 8 nm. The conformation of the pyrrolidine rings was of the mixed kind for each unit, i.e. A-E. The bonded potential of the pyrrolidine ring (including the two oxygen substituents) and the intrapyrrolidine non bonded potential was maintained hot with a scaling factor of 0.1 (corresponding to a temperature of about 3000 K) so as to lower the barrier between axial and equatorial conformation, thus enhancing the sampling efficiency of the system. All other bonded and non bonded intra and intermolecular interactions were unscaled thus evolving at a bath temperature of 300 K.

The simulation of the aggregates lasted for 10 nanoseconds and spontaneously evolved in a compact and relatively stable assembly with no apparent mesoscopic helicity and characterized by a large conformational pyrrolidinic disorder with mixing equatorial and axial structures for the substituents of the pyrrolidine ring. In Figure 1s (right) we show the time record of the gyration radius along with few snapshots evidencing the formation of the assembly (Figure 2s). The mean gyration radius, computed by standardly re-weighting the MD configurations (sampled discarding the first 4 ns of simulation) with the Umbrella bias potential for the pyrrolidine rings (i.e. by re-weighting each point with the factor $\exp(-V_b)$ with V_b being the bias intrapyrrolidine potential), is of about 1.41 nm and is shown in Figure 1s. In Figure 1s the (unbiased) distribution of the O-C-C-O dihedral angle is also reported (black curve). Axial (AA) and Equatorial (EE) conformations occur at 160 and 90 degrees, respectively. Both AA and EE conformations are present with a prevalence of the EE arrangements.

[8] Wang, J.; Wang, W.; Kollman P. A.; Case, D. A.. J. Mol. Graphics Model., **2006**, *25*, 247260.
[9] Singh, U.C.; Kollman, P.A. *J. Comp. Chem.* **1984**, *5*, 129
[10] Marsili, S.; Signorini, G. F.; Chelli, R.; Marchi, M.; Procacci, P. *J. Comp. Chemistry*, **2010**, *31*, 1106.

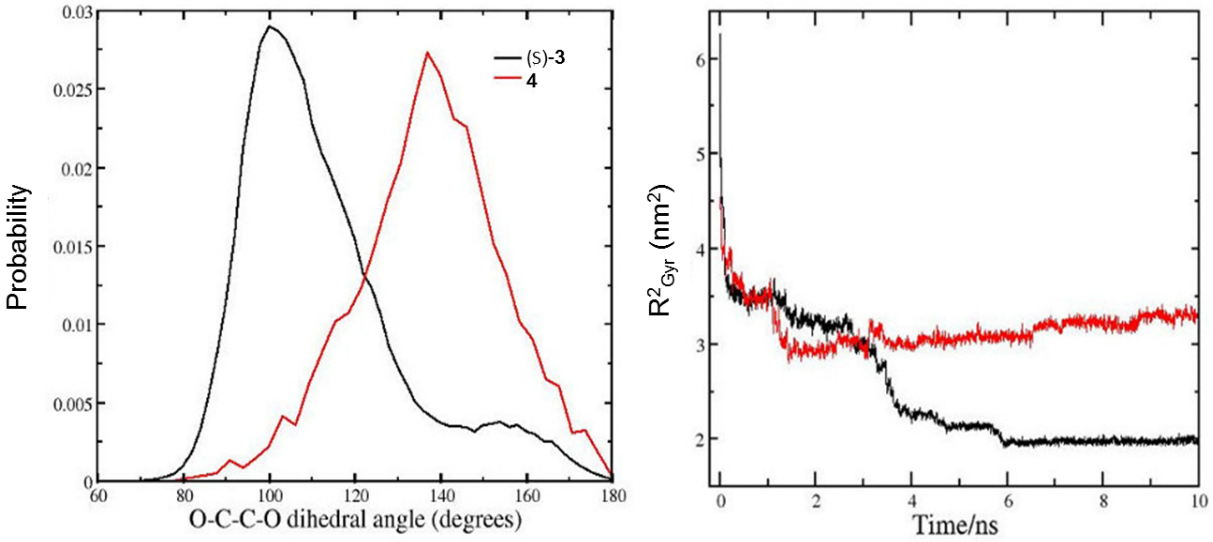

Figure 1s. Left: distribution of the intrapyrrolidine torsional angle in the assembly of pure (S)-**3** and in the mixture (S)-**3**+**4.** Right: Time record of the square of the radius of gyration for the hexadecamer of (S)-**3** (black) and of the mixture (S)-**3:4**, ratio1:8 (red).

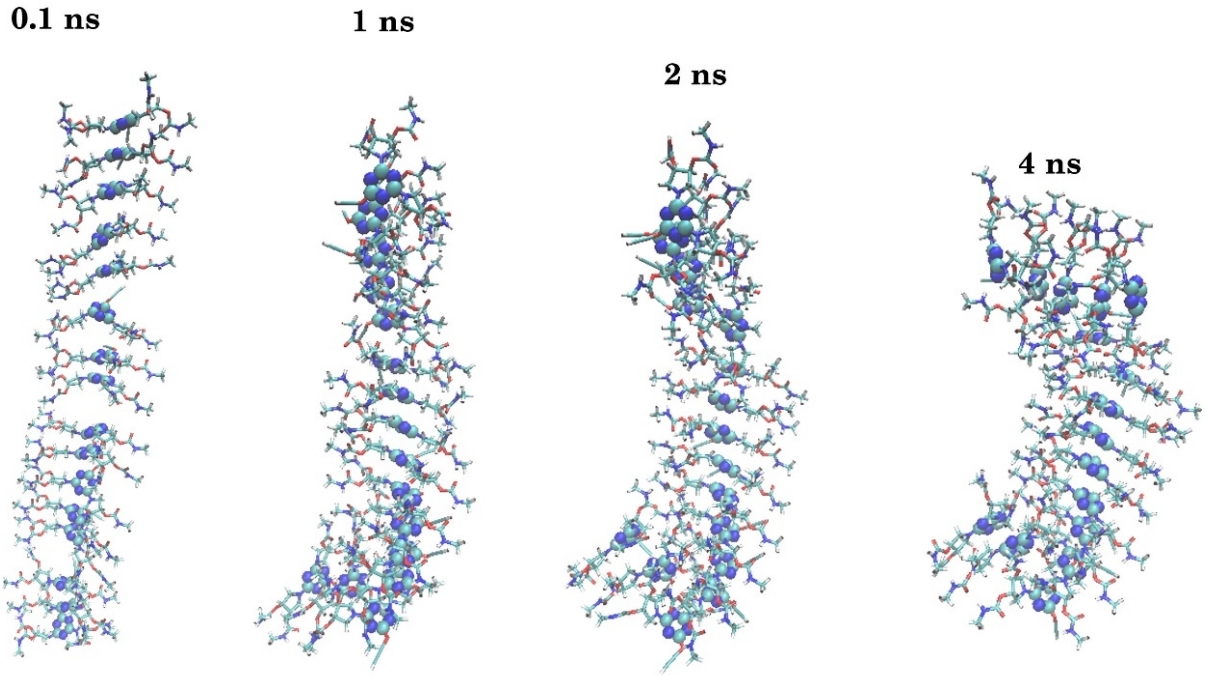

Figure 2s: Time evolution of the structure of the hexadecamer of (S)-**3** during the MD simulation at T=300 K *in vacuo*.

*Simulation of the mixed (S)-**3** + **4** aggregates.* The starting configuration was prepared from the starting pile structure of the hexadecamer of (S)-**3** units described above, by appropriately severing the intra-ring bond connecting the carbon atoms bearing the amide substituents for each unit except two of them (3rd and 14th unit in the stack). Prior to launch the simulation, the system underwent 100 cycles of conjugate gradient minimization for relaxing the structure after the pyrrolidine ring break-up according to GAFF force field. Again, in order to enhance the sampling efficiency, the intrapyrrolidine potential of the two (S)-**3** units was scaled with a factor of 0.1. The constant temperature simulation lasted for 10 nanosecond. The evolution of the system is shown in Figure 3s. Also in this case the system evolved quickly to a stable assembly

converging to a significantly larger radius of gyration with respect to the pure hexadecamer of (S)-**3** (see Figure 2s). The final bent structure of the 1:8 mixture is much more elongated and exhibits a right-handed helicoidal arrangement of the triazine chromophores, induced by the presence of the chiral (S)-**3** unit.
The mean radius of gyration (computed by reweighting with the Umbrella bias potential) is about 1.81 nm, i.e. 30% larger than the one obtained in the hexadecamer of pure (S)-**3**. The time evolution of the radius of gyration is reported in Figure 1s (right panel, red curve). At variance with what we observed in the hexadecamer of pure (S)-**3**, the two five (S)-**3** units in the mixture exhibit an (unbiased) distribution of the pyrrolidine torsional angle favouring the AA conformation.

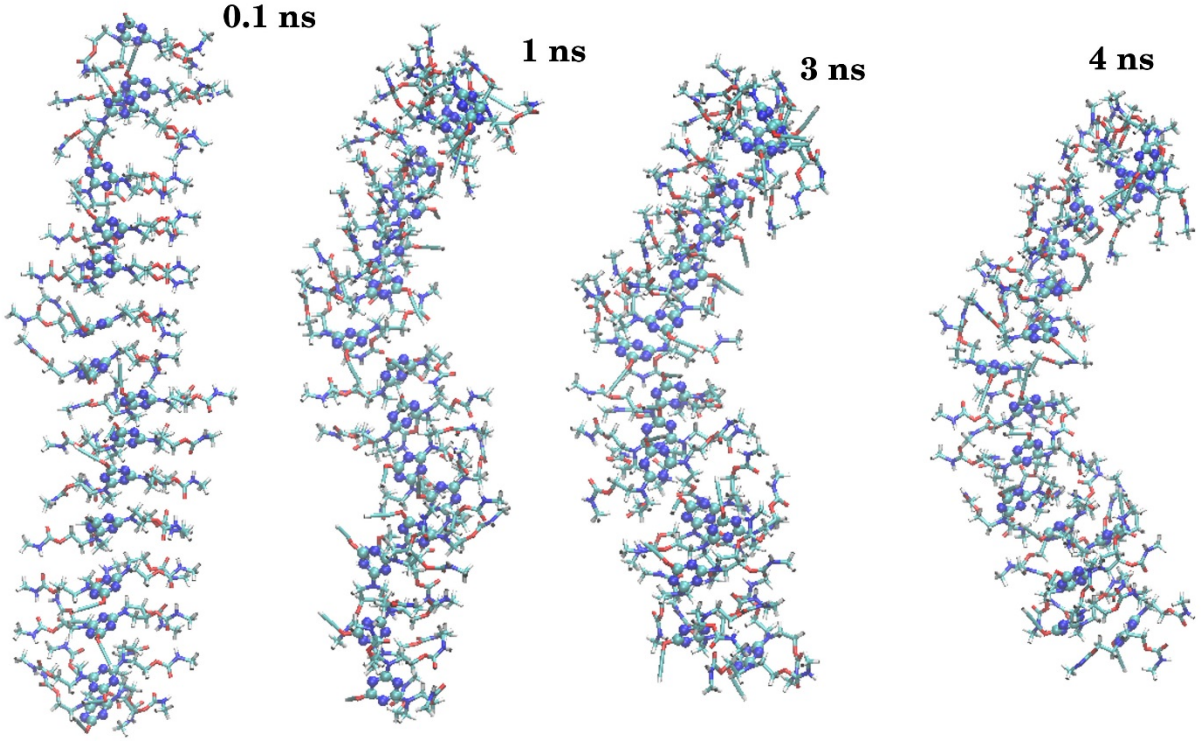

Figure 3s: Time evolution of the structure of the hexadecamer of (S)-**3:4** mixture during the MD simulation at T=300 K *in vacuo.*

Molecular modeling and CD calculations

Molecular mechanics and DFT calculations were run with Spartan'10 (Wavefunction, Inc., Irvine CA, 2010), with standard parameters and convergence criteria. TDDFT calculations were run with Gaussian'09,[11] with default grids and convergence criteria. Conformational searches were run with the Monte Carlo algorithm implemented in Spartan'10 using Merck molecular force field (MMFF). All MMFF minima within an energy window of 10 kcal/mol were optimized with DFT method at B3LYP/6-31G(d) level. Table 2s shows the DFT-calculated internal energies for all energy minima calculated for the truncated analog of compound (*S*)-**3**, with the dodecyl groups replaced by methyl groups.

[11] Gaussian 09, Revision C.01, Frisch, M. J.; Trucks, G. W.; Schlegel, H. B.; Scuseria, G. E.; Robb, M. A.; Cheeseman, J. R.; Scalmani, G.; Barone, V.; Mennucci, B.; Petersson, G. A.; Nakatsuji, H.; Caricato, M.; Li, X.; Hratchian, H. P.; Izmaylov, A. F.; Bloino, J.; Zheng, G.; Sonnenberg, J. L.; Hada, M.; Ehara, M.; Toyota, K.; Fukuda, R.; Hasegawa, J.; Ishida, M.; Nakajima, T.; Honda, Y.; Kitao, O.; Nakai, H.; Vreven, T.; Montgomery, Jr., J. A.; Peralta, J. E.; Ogliaro, F.; Bearpark, M.; Heyd, J. J.; Brothers, E.; Kudin, K. N.; Staroverov, V. N.; Kobayashi, R.; Normand, J.; Raghavachari, K.; Rendell, A.; Burant, J. C.; Iyengar, S. S.; Tomasi, J.; Cossi, M.; Rega, N.; Millam, J. M.; Klene, M.; Knox, J. E.; Cross, J. B.; Bakken, V.; Adamo, C.; Jaramillo, J.; Gomperts, R.; Stratmann, R. E.; Yazyev, O.; Austin, A. J.; Cammi, R.; Pomelli, C.; Ochterski, J. W.; Martin, R. L.; Morokuma, K.; Zakrzewski, V. G.; Voth, G. A.; Salvador, P.; Dannenberg, J. J.; Dapprich, S.; Daniels, A. D.; Farkas, Ö.; Foresman, J. B.; Ortiz, J. V.; Cioslowski, J.; Fox, D. J. Gaussian, Inc., Wallingford CT, 2009.

TDDFT calculations were run using CAM-B3LYP and B3LYP functionals, and TZVP and cc-pVDZ basis sets, leading to consistent results in all cases; the data discussed in the main text were obtained with CAM-B3LYP/TZVP including 16 excited states. CD spectra were generated from TDDFT calculations by applying a Gaussian band shape with 0.5 eV exponential half-width. Dipole-length rotational strengths were employed to construct CD spectra; the difference with dipole-velocity values was checked to be minimal for all relevant transitions. Average CD spectra were obtained by Boltzmann weighting of component spectra using populations estimated at 300K based on DFT-calculated internal energies.

DeVoe calculations were run with a Fortran routine due to Hug and coworkers.[12] It requires the description of all relevant electric transition dipoles in terms of position, polarization, transition frequency, dipole strength, and bandwidth. The input geometries were obtained from MD simulations on hexadecamers of (S)-**3**:**4** mixtures discussed previously, by cutting the 4 final molecules from each end and retaining the central portion constituted by octamers of **4**. Several input structures were considered obtained from different MD snapshots randomly chosen after convergence of MD simulations. The first three π–π* transitions for each triazine ring were included in the calculation. The transition dipoles were placed in the middle of the N5–C2(O) distance of each ring. Transition parameters and polarization directions are reported in Table 3s and were derived from the UV-vis absorption spectrum of compound (S)-**3** in cyclohexane and from TDDFT calculations.

[12] Cech, C. L.; Hug, W.; Tinoco, I. Jr. *Biopolymers* **1976**, *15*, 131−152.

Conformer	E (au)	Geometry[a]	rel. E (kcal/mol)	Note
#1	-1986.42633	AA	0	(b)
#2	-1986.42626	AA	0.04	
#3	-1986.42576	AA	0.36	
#4	-1986.42563	AA	0.44	
#5	-1986.42499	EA	0.84	
#6	-1986.42488	EA	0.91	
#7	-1986.42481	AE	0.95	(c)
#8	-1986.42472	EA	1.01	
#9	-1986.42470	AE	1.02	
#10	-1986.42459	AE	1.09	
#11	-1986.42457	AE	1.10	
#12	-1986.42457	AE	1.10	
#13	-1986.42446	AE	1.17	
#14	-1986.42436	EE	1.23	(d)
#15	-1986.42351	EE	1.77	
#16	-1986.42327	EE	1.92	
#17	-1986.42323	EE	1.94	
#18	-1986.42285	EE	2.18	
#19	-1986.42044	AE	3.69	
#20	-1986.42027	EE	3.80	
#21	-1986.41987	EE	4.05	
#22	-1986.41965	EE	4.19	
#23	-1986.41949	EE	4.29	
#24	-1986.41940	EE	4.34	
#25	-1986.41921	EE	4.46	
#26	-1986.41910	EE	4.54	

Table 2s. DFT-optimized (B3LYP/6-31G(d) level) structures for the truncated analog of compound (*S*)-**3** with respective internal energies.

(a) Orientation of the carbamate substituents on the pyrrolidine ring: A: axial; E: equatorial. (b), (c), (d) shown in figure 2b (main text).

Transition	Wavelength (nm)	Frequency (1000 cm^{-1})	Dipole strength (square Debye)	Bandwidth (1000 cm^{-1})	Polarization [(a)]
1	240	41.7	1.5	3.0	long
2	220	45.4	50	3.0	short
3	217	46.1	8	3.0	long

Table 3s. Transition parameters used for DeVoe calculations, determined as described in the text.

(a) See below.

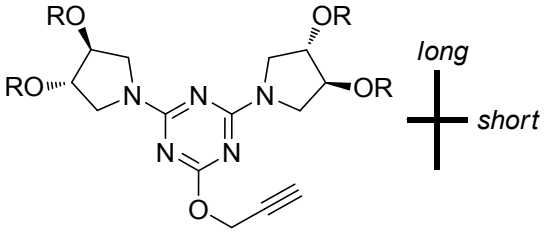

Compound **2** ^{1}H-NMR

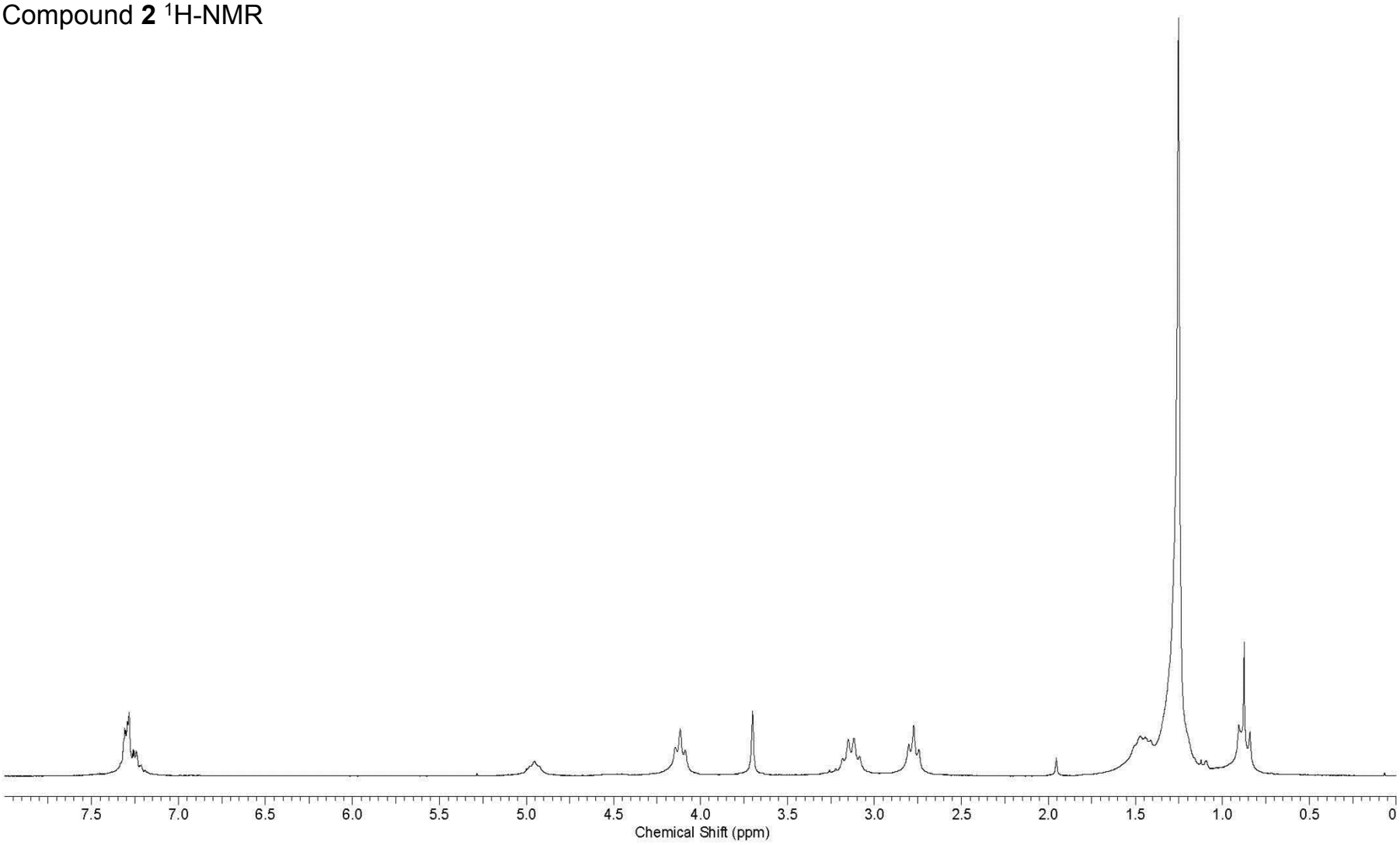

Compound **2** ^{13}C-NMR

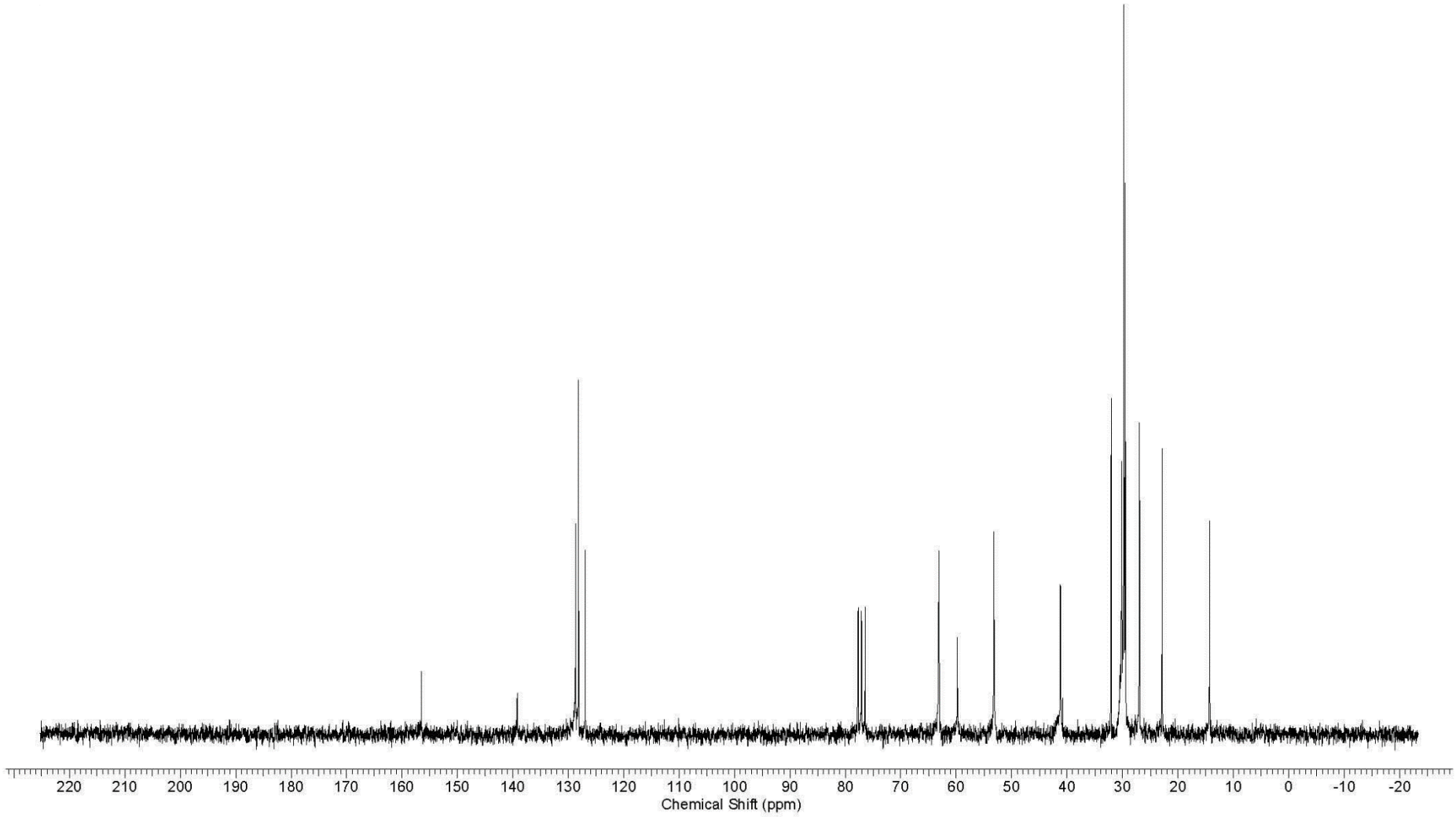

Compound **4** ^{1}H-NMR

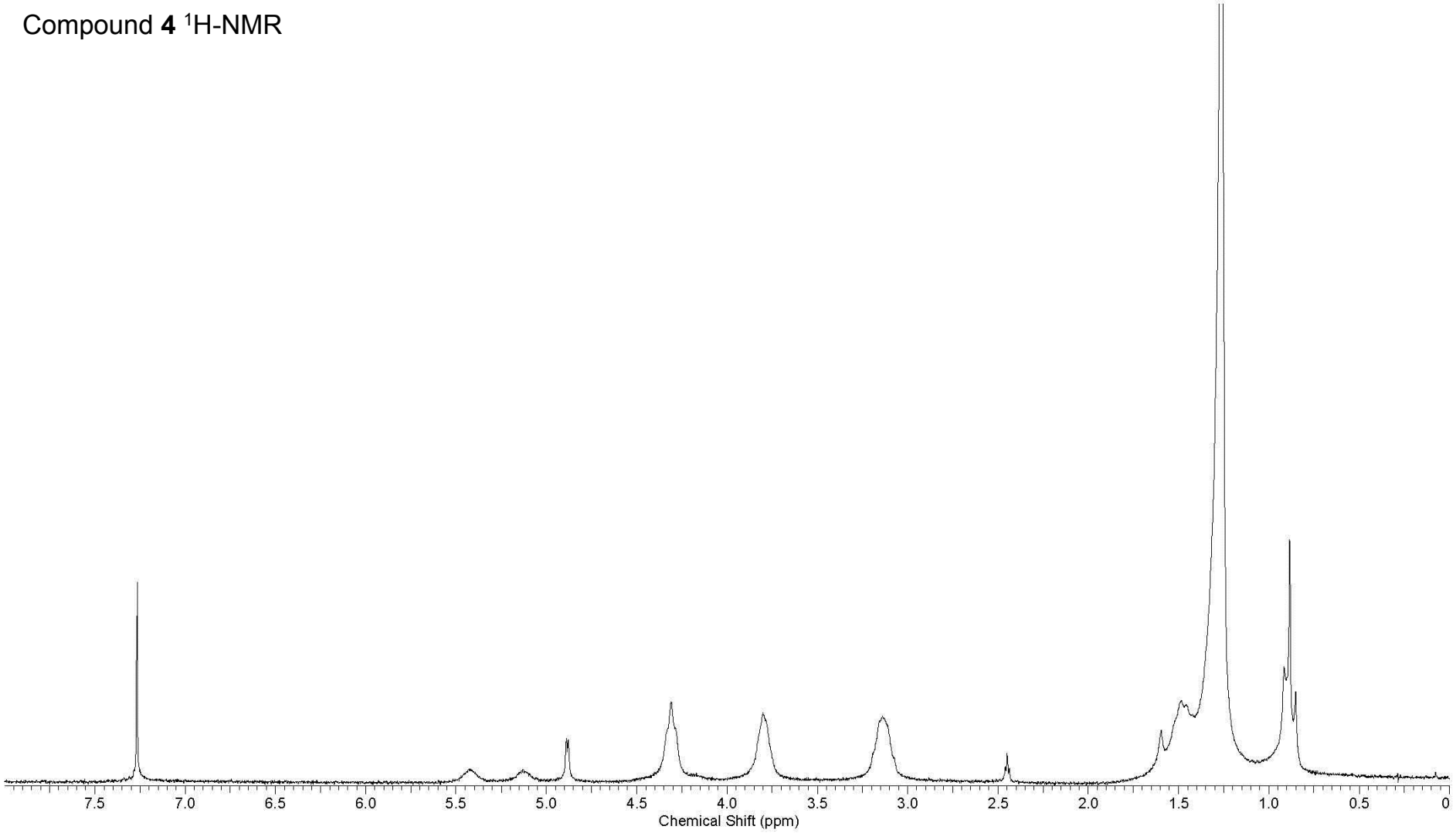

Compound **4** ^{13}C-NMR